CP-PACS results for quenched QCD spectrum with the Wilson action *

CP-PACS Collaboration

S. Aoki[a], G. Boyd[b], R. Burkhalter[b], S. Hashimoto[c], N. Ishizuka[a], Y. Iwasaki[a,b], K. Kanaya[a,b], Y. Kuramashi[c], M. Okawa[c], A. Ukawa[a], T. Yoshié[a,b]

[a]Institute of Physics, University of Tsukuba, Tsukuba, Ibaraki 305, Japan

[b]Center for Computational Physics, University of Tsukuba, Tsukuba, Ibaraki 305, Japan

[c]High Energy Accelerator Research Organization (KEK), Tsukuba, Ibaraki 305, Japan

We present progress report of a CP-PACS calculation of quenched QCD spectrum with the Wilson quark action. Light hadron masses and meson decay constants are obtained at $\beta =$ 5.9, 6.1, and 6.25 on lattices with a physical extent of 3 fm, and for the range of quark mass corresponding to $m_\pi/m_\rho \approx 0.75 - 0.4$. Nucleon mass at each β appears to be a convex function of quark mass, and consequently the value at the physical quark mass is much smaller than previously thought. Hadron masses extrapolated to the continuum limit exhibits a significant deviation from experimental values: with K meson mass to fix strange quark mass, strange meson and baryon masses are systematically lower. Light quark masses determined from the axial Ward identity are shown to agree with those from perturbation theory in the continuum limit. Decay constants of mesons are also discussed.

1. Introduction

Precision determination of the light hadron spectrum is a fundamental problem of lattice QCD. Over the years numerous studies have been carried out on this subject, which have revealed a number of difficulties that have to be overcome to achieve this goal. In addition to the overriding issue of how quenching distorts the spectrum, calculations aiming at precise results have to have good control over the systematic errors arising from a finite spatial lattice size, an extrapolation toward light quark masses, and an extrapolation to the continuum limit. There is also the issue of how reliably one can extract hadron masses from the propagators whose statistical errors generally grow exponentially with the distance from the source point.

Within quenched QCD high statistics calculations on large lattices attempting to deal with these problems gradually developed since around 1990 exploiting the power of dedicated parallel computers[1–5]. In particular Weingarten and collaborators with the GF11 computer carried out a pioneering work on the continuum limit of the quenched spectrum with extensive simulations including finite size studies[3]. In spite of these efforts convincing results on hadron masses in quenched QCD with a precision reliably better than 5% have not been obtained. In particular the question in what way the quenched spectrum deviates from the experiment has not been fully answered so far.

In view of this situation the CP-PACS Collaboration has decided to undertake a quenched simulation of the light hadron spectrum as the first lattice QCD project of the CP-PACS computer which started operation in April 1996. The strategy we have chosen is to employ the simplest form of the action, *i.e.,* the plaquette action for gluons and the Wilson action for quarks, and carry out, as much as the computing power of CP-PACS allows, a measurement of hadron masses down to small quark masses at small lattice spacings employing large lattices and high statistics. The simulation has been running since the summer of

---

1996 and are still continuing. In this article we report the present status of the work.

2. Parameters of simulation

In Table 1 we list the parameters chosen for our simulation, and the number of configurations for hadron mass measurements accumulated as of the time of the Workshop.

We choose four values of the coupling constant β to cover the range of lattice spacing $a^{-1} \approx 2 - 4$ GeV for controlling scaling violation effects and taking the continuum limit. In order to avoid finite size effects, the spatial lattice size L is chosen so that the physical size equals approximately 3 fm. The temporal lattice size is set equal to $7L/4$; this choice is based on considerations on length of time intervals needed for a reliable extraction of masses with an exponentially smeared source we employ for hadron mass measurements.

For each value of β we select five values of the hopping parameter such that the ratio m_π/m_ρ takes values of about 0.75, 0.7, 0.6, 0.5, and 0.4. We abbreviate these hopping parameters as s_1, s_2, u_1, u_2 and u_3. The first two values are for interpolation of results to strange quark, and the rest are for examining chiral extrapolation. Previous spectrum studies with the Wilson quark action have been limited to the range $m_\pi/m_\rho \geq 0.5$. The value $m_\pi/m_\rho \approx 0.4$ represents our attempt toward lighter quark masses. Reducing the quark mass further is not easy: test runs we have carried out for $m_\pi/m_\rho \approx 0.3$ at $\beta = 5.9$ show that fluctuations large and that it takes more computer time than that for the five hopping parameters down to $m_\pi/m_\rho \approx 0.4$. We calculate hadron masses for equal mass cases and also for the unequal mass cases of the type $s_i u_j$ for mesons and $s_i s_i u_j$ and $s_i u_j u_j$ for baryons.

Configurations are generated with the 5-hit Cabibbo-Marinari-Okawa heat-bath algorithm and the over-relaxation algorithm mixed in the ratio of 1:4. The combination is called a sweep, and we skip 200 to 2000 sweeps between hadron mass measurements as listed in Table 1.

Quark propagators are solved with the red/black-preconditioned minimal residual algorithm imposing the periodic boundary condition in all four directions. The stopping condition is chosen to ensure that truncation error in hadron propagators is at most 5 percent of our estimated final statistical error. For performance of our code on the CP-PACS see Refs. [6,7]

Errors are estimated by a single elimination jackknife procedure.

We note that results presented here are preliminary, as runs are still continuing. In particular the run at $\beta = 6.47$ has been just started. Although some figures include results at $\beta = 6.47$, values in the continuum limit are determined by extrapolating data at the first three values of β.

3. Extraction of hadron masses

3.1. Smearing

We employ an exponential smearing of quark source to enhance signals of ground state in hadron propagators. This choice is motivated by a recent measurement of the pion wave function defined by $\psi(r) = \langle 0| \sum_x \bar{q}(x)\gamma_5 q(x + r)|\pi\rangle/\langle 0| \sum_x \bar{q}(x)\gamma_5 q(x)|\pi\rangle$ by the JLQCD Collaboration, who found that $\psi(r)$ is well reproduced by a single exponential function: $\psi(r) = A \exp(-Br)$[8].

To choose the value of the slope B in our measurement, we parameterize their results in the form $B(m_\rho, m_q) = (x_0 + x_1 \cdot m_\rho) + (y_0 + y_1 \cdot (m_\rho)^2) \cdot m_q$. Estimates from available data for the value of m_ρ appropriate for our simulation parameters are then substituted to find the value of B. The smearing radius $1/B$ chosen in this way does not vary much over the points of our simulation, being approximately given by $1/B \approx 0.33$ fm.

Various combinations of point (P) and smeared (S) sources are used to construct hadron operators at the source. In the following we employ a notation such as PSS to specify the combination of quark sources. On the other hand, we always use point sinks for hadron operators at the sink.

In Fig.1 we show typical results of effective masses for various source combinations. We find that the effective mass reaches a plateau from above in almost all cases for all combinations of source. This suggests that the smearing radius of $1/B \approx 0.33$ fm we choose is smaller than the actual spread of hadron wave functions.

Table 1
Simulation parameters. Values of a^{-1} are determined from m_ρ.

β	size	a^{-1} (GeV)	La (fm)	#conf	sweep /conf	hopping parameter
5.90	$32^3 \times 56$	1.96(2)	3.23(3)	674	200	0.15660, 0.15740, 0.15830, 0.15890, 0.15920
6.10	$40^3 \times 70$	2.58(3)	3.06(3)	384	400	0.15280, 0.15340, 0.15400, 0.15440, 0.15460
6.25	$48^3 \times 84$	3.10(4)	3.05(4)	262	1000	0.15075, 0.15115, 0.15165, 0.15200, 0.15220
6.47	$64^3 \times 112$	4.19(12)	3.01(8)	22	2000	0.14855, 0.14885, 0.14925, 0.14945, 0.14960
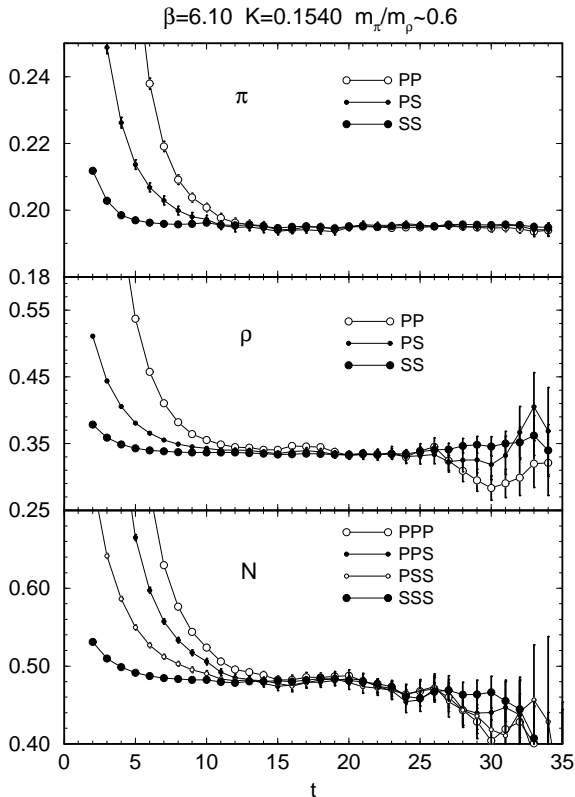
Figure 1. Typical results of effective masses obtained with various combinations of quark sources.

we therefore decide to derive masses from the SS source for mesons and the SSS source for baryons.

To extract hadron masses from propagators we employ a single hyperbolic cosine fit for mesons and a single exponential fit for baryons. The largest time slice of the fit $t_{\max}$ is chosen by the requirement that the error of propagator does not exceed 5%. Changing the minimum time $t_{\min}$ of the fit, we compare results of correlated and uncorrelated fits. We find that 1) χ^2/N_{DF} for correlated fit decreases as $t_{\min}$ increases and becomes constant at some time slice called t_χ[2]. 2) For $t_{\min} \geq t_\chi$, mass results from correlated and uncorrelated fits agree within at most 1.5 standard deviations. 3) Uncorrelated fits give results more stable as a function of $t_{\min}$. From these investigations, we decide to adopt mass results from the uncorrelated fit at $t_{min} \approx t_\chi$, supplememted with a single elimination jackknife analysis to estimate the error of masses. We consider that the magnitude of systematic error due to the choice of fitting ranges and fitting procedure is comparable to statistical error.

In Table 2, we list typical statistical errors in mass results in units of percent, which are estimated by the single elimination jackknife method. In the contiuum limit results for the nucleon has the largest error of about 5% with present statistics.

3.2. Fitting Procedure

We observe in Fig. 1 that the onset of plateau is earliest if the smeared source is used for all quark and antiquark fields in hadron operators. Furthermore statistical errors of effective masses at a given time slice are the smallest for this combination. For results presented in this report,

4. Extrapolation and interpolation to physical quark mass

Our first interest is how hadron masses depend on the quark mass. We start with the pseudo scalar case, and plot in Fig.2 the ratio $m_\pi^2/[(m_1 + m_2)/2]$ against $(m_1 + m_2)/2$, where m_i are quark masses defined by $m_i = Z_m(1/K_i - 1/K_c)$. Con-

4

Table 2
Errors in mass results in units of percent.

	π	ρ	N	Δ
s_1	0.1	0.2	0.3	0.3
s_2	0.1	0.3	0.3	0.4
u_1	0.2	0.4	0.5	0.5
u_2	0.3	0.6	0.7	0.6
u_3	0.4	0.8	0.9	0.7
K_c		1.2	2.0	1.0
$a = 0$			5.5	3.7
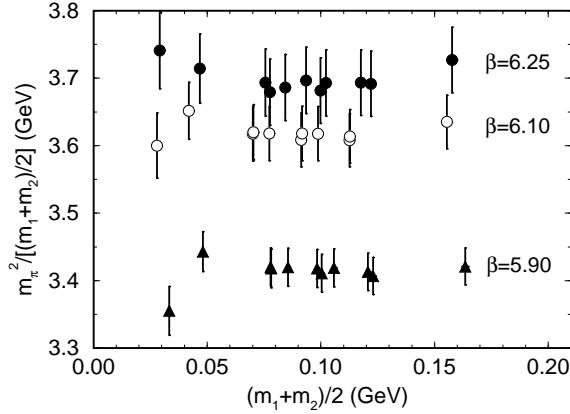
Figure 2. $m_\pi^2/[(m_1+m_2)/2]$ as a function of $(m_1+m_2)/2$.

Figure 3. Pseudo-scalar meson masses squared and vector meson masses as functions of $1/K$ of light quark.

version to physical units is made with estimates of lattice spacing in terms of m_ρ as described below. The critical hopping parameter K_c is determined by a linear extrapolation of m_π^2, and Z_m denotes the one-loop renormalization factor (see sec.6 for details). The ratio for 11 combinations of quark masses is constant within errors at each β. Therefore we conclude that the pseudo scalar meson mass squared is linear in the average quark mass in the range covered by our data. In other words, we find no clear evidence for the existence of chiral perturbation theory higher order terms or quenched chiral logarithms[9] in the results of pseudo scalar meson masses down to $m_q \approx 30$ MeV.

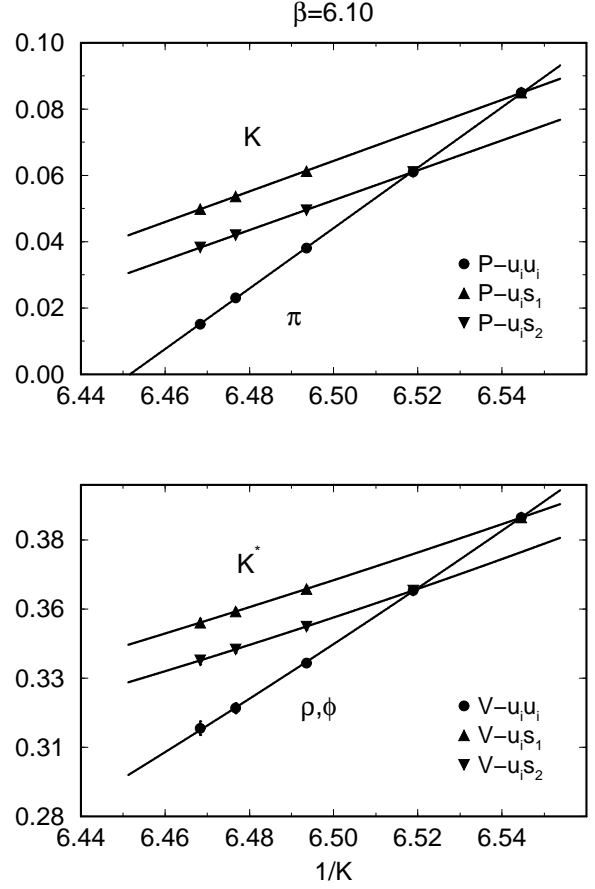Vector mesons and decuplet baryons also exhibit the property that their masses are linear in the average of quark masses with only a small mixture of higher order terms. This is illustrated in Fig.3 and 4 in which hadron masses are plotted against $1/K$ of lighter quark, together with results of a linear (pseudo scalar case) or quadratic (vector and decuplet case) fit.

However, this property is badly broken for octet baryons as shown in Fig.5. Although Σ and Ξ masses are linear in $1/K$, nucleon and Λ masses are convex. The nucleon mass at the lightest quark mass is clearly off the linear fit (dashed line) as compared to a cubic fit shown by a solid line.

In this connection we show our results for m_N/m_ρ as a function of m_π/m_ρ in Fig.6. Dotted

β=6.10

β=6.10

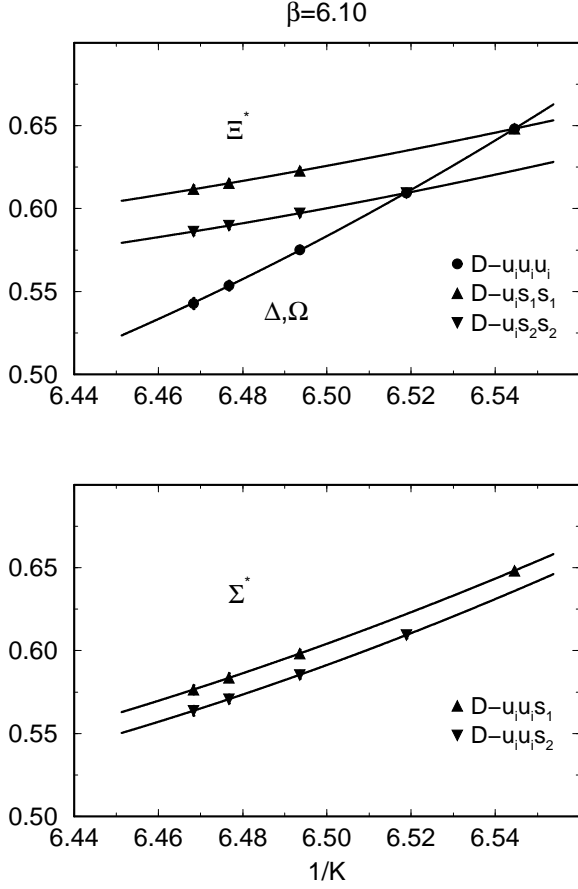Figure 4. Decuplet baryon masses against $1/K$ of light quark.

Figure 5. Octet baryon masses against $1/K$ of light quark.

and thick curves correspond to the cases in which the nucleon mass at $\beta = 6.25$ is fitted with a linear or cubic functions of quark mass, respectively. Higher order terms are essential in order to make a reliable extrapolation of nucleon and Λ masses to the chiral limit, and have a significant impact on final results.

Based on the considerations described above, we employ a linear fit for pseudo-scalar mesons, cubic fit for nucleon and quadratic fit for other hadrons in order to extrapolate or interpolate hadron mass results to physical quark masses at each β. For vector mesons a linear fit reads to essentially the same result. We then determine values of $K_{u,d}$ and a^{-1} taking the experimental
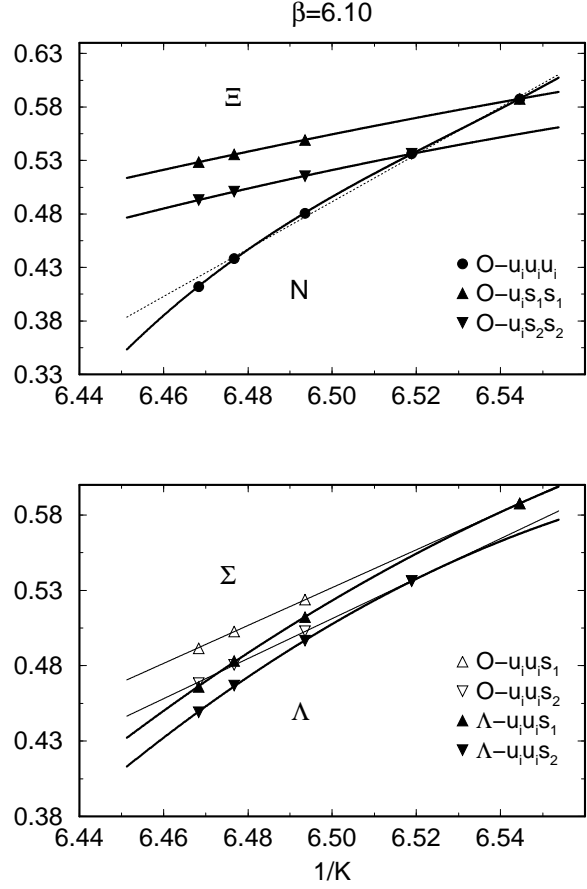
values of m_π and m_ρ. The hopping parameter K_s for strange quark is estimated in two ways, either from m_ϕ assumed to be a pure $\overline{s}s$ state or from m_K or m_{K^*}. For the latter case we take meson mass data for unequal quark masses and first make an extrapolation of lighter quark to $K_{u,d}$ with the heavier quark fixed at s_1 and s_2. We then linearly interpolate the result so that K or K^* meson mass has the experimental value. For experimental values we use $m_\pi = 135$ MeV, $m_\rho = 769$ MeV, $m_\phi = 1019$ MeV, $m_K = 498$ MeV, and $m_{K^*} = 896$ MeV.

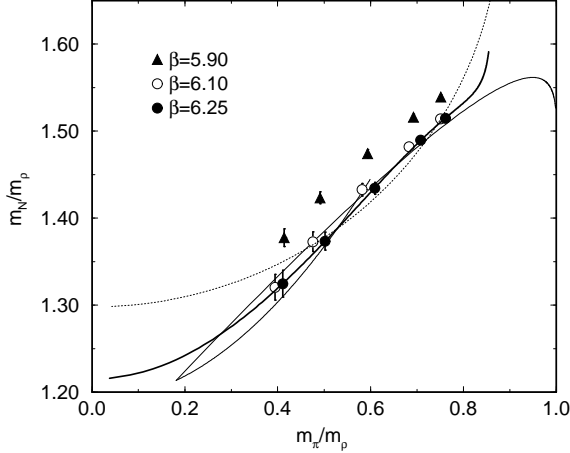## 5. Quenched hadron spectrum in the continuum limit

Figure 6. Edinburgh plot showing m_N/m_ρ as a function of m_π/m_ρ. For explanation of lines see text.

5.1. Scale parameter

The scale parameter Λ is a fundamental quantity in QCD. We estimate the value in the $\overline{MS}$ scheme defined by

$$\Lambda_{\overline{MS}} = \frac{\pi}{a}(b_0 g_{\overline{MS}}^2(\pi/a))^{-b_1/2b_0^2} e^{-1/2b_0 g_{\overline{MS}}^2(\pi/a)}.$$

where for the $\overline{MS}$ coupling we employ the tadpole-improved one-loop formula given by[10, 11]

$$1/g_{\overline{MS}}^2(\pi/a) = \mathrm{tr}(U_P/3)/g^2 + 0.02461.$$

We show the result in Fig.7(a) as a function of $m_\rho a$. Our results are consistent with those reported so far [2–4,1] for the Wilson action. Our errors, however, are much reduced. In Fig.7(b) are compared our results with those for the Kogut-Susskind action[12] and those from string tension[13]. We find that all of the results agree in the continuum limit.

5.2. Strange mesons

In Fig.8 we show the continuum extrapolation for masses of mesons containing a strange quark. We find a linear behavior of the masses in lattice spacing to be well satisfied as shown by solid lines.

As we noted in Sec. 4 strange quark mass can be determined in two ways. In Fig.8(a) we take m_K as input and predict the masses of ϕ and K^*
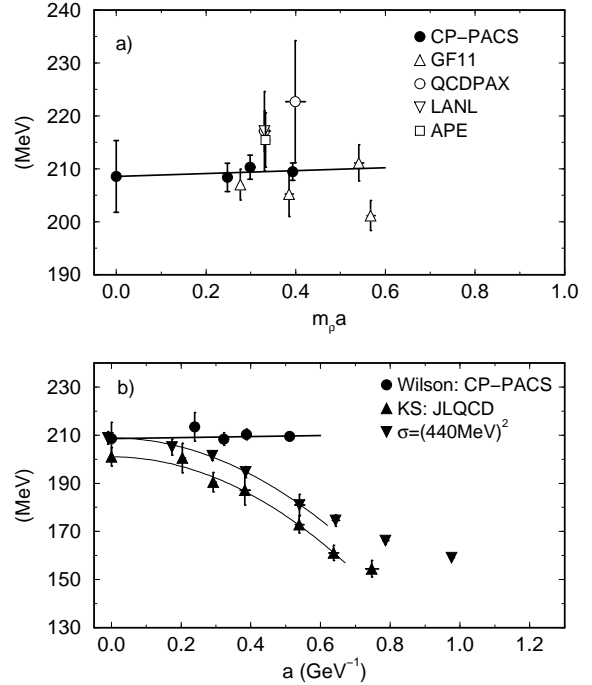

Figure 7. $\Lambda_{\overline{MS}}$ vs. $m_\rho a$ (top figure) and a^{-1} (bottom figure). Data for Wilson quarks are taken from GF11[3], QCDPAX[2], LANL[4], and APE[1]. Data for the KS action are from ref.[12]. Data for the string tension are taken from ref.[13].

meson. The values extrapolated to the continuum disagree with experimental values plotted by open circles at $a = 0$.

This should be contrasted with the results of the GF11 Collaboration[3] plotted by open squares. They linearly extrapolate data measured on lattices with a spatial extent of about 2.3 fm (dashed lines). They then make a finite size correction to the extrapolated value, and obtain a result which agree well with experiment. The best fit to our data differ from those by GF11 taken on a 2.3 fm lattice, while their data on a 3.3 fm lattice at $\beta = 5.7$ are consistent with a linear fit of our results.

We show an alternative procedure in Fig.8(b) where we plot results for m_K and m_{K^*} when we take m_ϕ as input. In this case, the value of m_{K^*} in the continuum limit is consistent with experiment, while that for m_K is much higher. These
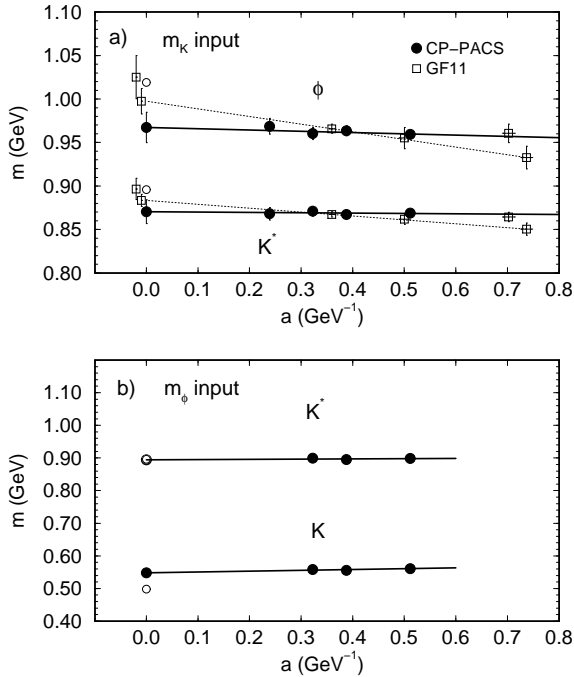
Figure 8. Strange meson masses and their extrapolations to the continuum limit. Open circles represent experimental values. Data from GF11[3] are plotted by open squares for comparison.

Figure 9. Value of J vs. $m_\rho a$. Data are taken from references quoted in the caption of Fig. 7 and refs. [15,16]. We have calculated values of J using data of m_π and m_ρ in the cases that values of J are not reported in the literature.

results mean that there are no choice of strange quark mass which leads to an agreement of vector as well as pseudo-scalar meson masses.

The J parameter[14] is a convenient quantity to summarize the situation. As shown in Fig.9(a), the value of J in the continuum limit is smaller than the experimental value by more than 2 standard deviations. In Fig.9(b), we compare our results with those obtained with the Kogut-Susskind quark action[12] and the clover quark action[16]. In the continuum limit, the two actions give a result consistent with that of the Wilson action.

5.3. Baryon masses

Our results for nucleon and Δ masses are shown in Fig.10(a). For the nucleon our continuum extrapolated value is about 5% smaller than experiment. While the difference is only a one standard deviation effect, this contrasts with experience of
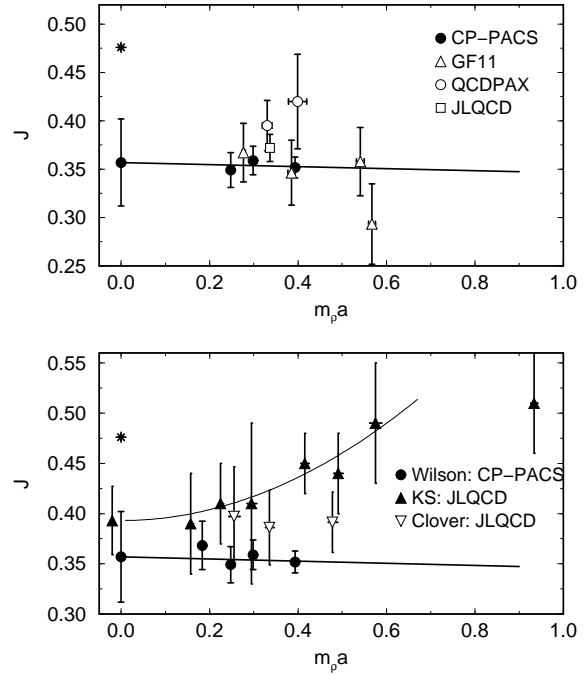
previous studies that the nucleon mass tends to come out higher than experiment. In fact our results are significantly lower already at finite lattice spacings compared with previous results also shown in the figure. The discrepancy is mainly due to the bending of the nucleon mass toward small quark masses as discussed in Sec. 4.

We emphasize that our results are consistent with those from other groups in the region of strange quark. If we make a linear chiral extrapolation of the nucleon mass employing only three points of our data corresponding to $m_\pi/m_\rho \approx$ 0.75, 0.7, and 0.6, we obtain results in the chiral limit which agrees with those reported so far as illustrated in Fig.10(b).

For Δ results from the present work and those of earlier studies overlap at finite lattice spacing. Nonetheless the continuum extrapolation leads to a value about 5% larger compared to experiment
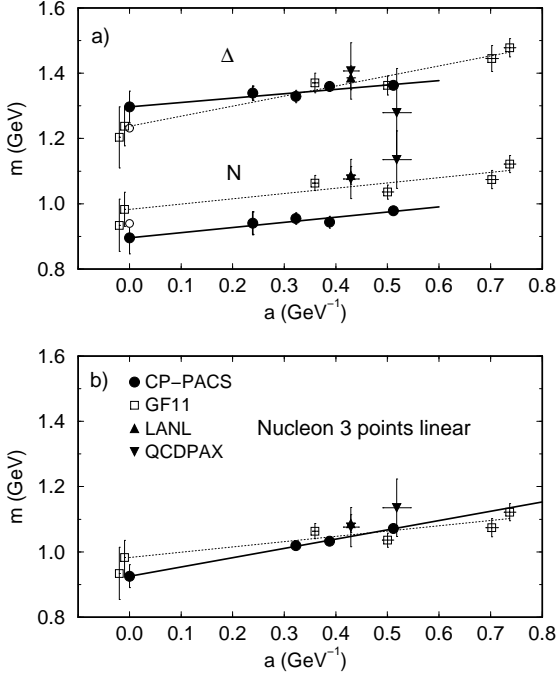
Figure 10. (a) The same as Fig.8 for nucleon and Δ. (b) Nucleon masses obtained by linear fits to data at the largest three quark masses.

in our case as compared to a value consistent with experiment reported by GF11.

Figure 11 shows results for strange baryons employing m_K to determine the strange quark mass. We observe significant departures from the experiment except for Σ^*. Our extrapolation is quite different from that of GF11 for Ω and Ξ^* for which GF11 found an agreement with the experiment.

5.4. Quenched spectrum of light hadrons

We show all of our results for the quenched light hadron spectrum in Fig. 12 where we also plot the experimental spectrum (horizontal dashed bars) and the results of GF11 (open symbols) for comparison. For strange quark mass the K meson mass is used as input both in our results and those of GF11.

It is quite conspicuous that the masses of baryons containing strange quark are systematically lower than experiment. This may be related to a similar deviation in the meson sector where
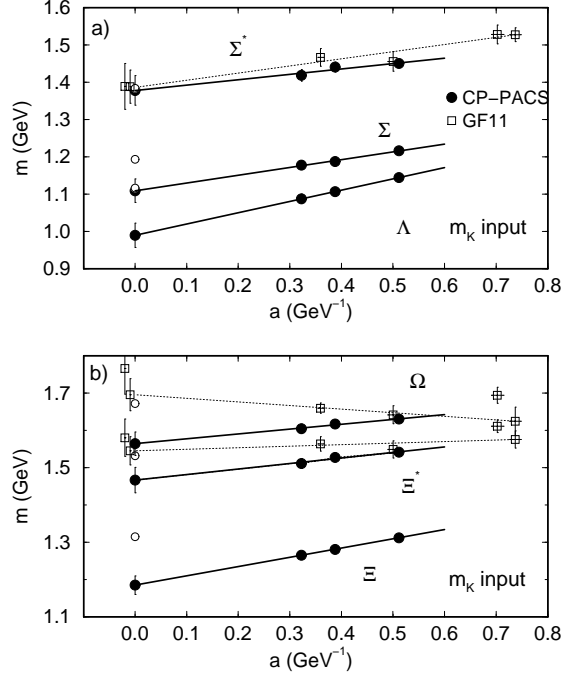

Figure 11. The same as Fig.8 for strange baryons.

the masses of K^* and ϕ are smaller.

It is interesting to note that agreement with experiment is much better if we examine the spectrum within each flavor $SU(3)$ multiplet. For example, if we take m_ρ and m_ϕ to determine the lattice spacing and the strange quark mass, mass of K^* is consistent with experiment, and a similar situation holds for Σ^* and Ξ^* masses if we take the Δ and Ω masses instead for input. This property may contain some hint to consider the problem of how dynamical quark effects correct the discrepancy observed in Fig. 12.

In the up-down quark sector our value for the nucleon mass is smaller than experiment by about 5% and that for Δ larger by a similar amount. The errors are of a similar magnitude, however.

Compared to the results of GF11, our errors are reduced by a factor two with our present statistics. The spectrum itself deviate from that of GF11 beyond estimated errors in a number of channels, most notable being ϕ, Ξ^* and Ω.
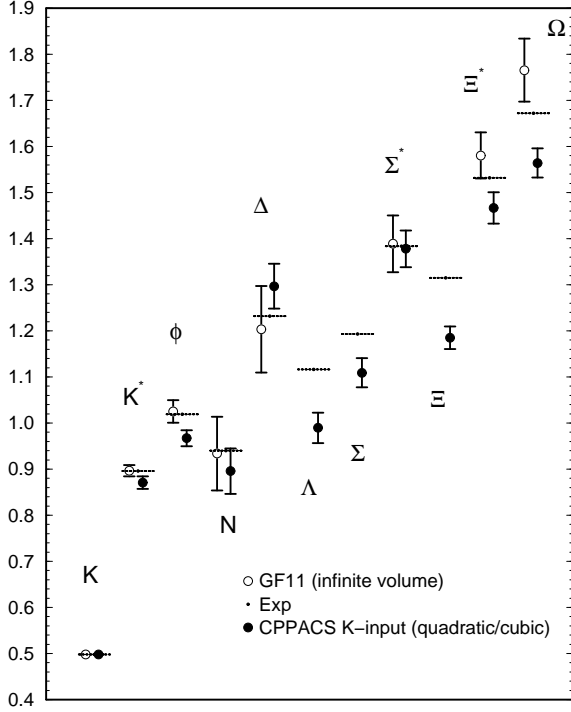
Figure 12. Results for the quenched light hadron spectrum in the continuum limit from the present work as compared with experimental spectrum (horizontal dashed bars) and those of GF11 (open circles).

6. Light quark masses

The values of light quark masses are important in a variety of phenomenological context[17]. Perturbatively quark mass is defined by

$$2m_q^{\text{Pert.}} = Z_m(1/K_1 + 1/K_2 - 2/K_c) \qquad (1)$$

with a renormalization factor Z_m. A non-perturbative definition is also possible based on the axial vector Ward identity[18–20]

$$\langle 0|\partial_\mu A_\mu|x\rangle = 2m_q \langle 0|P|x\rangle. \qquad (2)$$

We take here the definition given by

$$2m_q^{\text{PCAC}} = -m_\pi \frac{Z_A}{Z_P} \lim_{t\to\infty} \frac{\sum_{\vec{x}}\langle A_4(\vec{x},t)\ P\rangle}{\sum_{\vec{x}}\langle P(\vec{x},t)\ P\rangle}, \quad (3)$$

where A_4 is the local axial current and P is the pseudo-scalar density, and m_π on the righthand
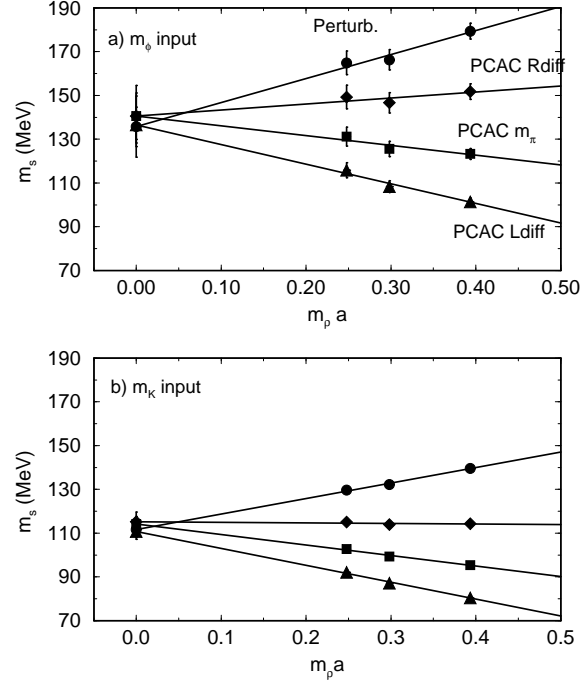

Figure 13. Strange quark masses in the $\overline{MS}$ scheme at $\mu = 2$ GeV obtained from perturbation theory and from the axial Ward identity. Rdiff(Ldiff) stands for right- (left-) difference for an approximation to the time derivative in the Ward identity. Values obtained with center-difference are numerically close to those with m_π, and are omitted in the figure.

side is an approximation to the time derivative in the Ward identity.

We compare results for the two definitions of quark mass. For the Ward identity method we test also $e^{m_\pi} - 1$, $1 - e^{-m_\pi}$, and $(e^{m_\pi} - e^{-m_\pi})/2$ instead of m_π for replacing the time derivative which correspond to right-, left- and center-difference, respectively. For the renormalization constants Z_m[21], Z_A and Z_P[22], we employ one-loop results improved by the tadpole procedure with the coupling $\alpha_V(1/a)$ [10]given by $Z_m = 8K_c(1 + 0.01\alpha_V(1/a))$, $Z_P = Z_K(1 - 1.034\alpha_V(1/a))$, and $Z_A = Z_K(1 - 0.316\alpha_V(1/a))$. Matching of lattice values of quark mass to those in the continuum is made at the scale $1/a$ employing the $\overline{MS}$ scheme in the continuum. The
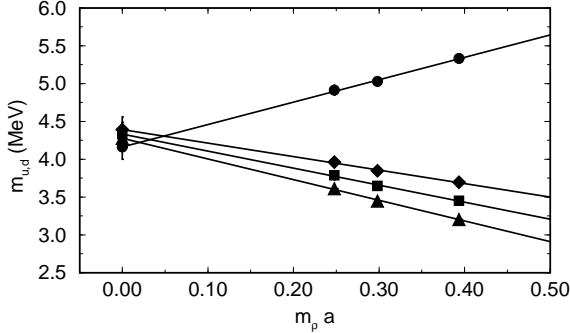
Figure 14. The same as Fig.13 for the average of up and down quark masses.

result is then run by the two-loop renormalization group equation to 2 GeV.

We plot results for the strange quark mass obtained with perturbative and three cases of non-perturbative PCAC definitions in Fig.13. The ϕ meson mass is used to determine K_s in Fig.13(a) and the K meson mass is employed in (b). For finite lattice spacings the four definitions yield significantly different values. However, a linear extrapolation yields results in mutual agreement in the continuum limit. The same situation also holds for the average of up and down quark mass as shown in Fig.14.

We note, however, that the value $m_s \approx 140$ MeV for the strange quark mass in the continuum limit obtained with m_ϕ as input does not agree with $m_s \approx 115$ MeV found with m_K as input. This is another sign of pathology in quenched QCD.

In Fig.15, we compare our results for perturbative quark masses with those from other groups[8,2–4]. Extrapolating our data to the continuum limit leads to $m_{u,d} \approx 4.2$ MeV and $m_s \approx 136$ MeV. They are larger than the values estimated in Ref.[23] ($m_{u,d} \approx 3.4$ MeV and $m_s \approx 96$ MeV) based on a compilation of world data for the Wilson action. In the same figure we also plot results for the Kogut-Susskind action obtained by the JLQCD collaboration[12]. It is not clear if Wilson and Kogut-Susskind results agree in the continuum limit.
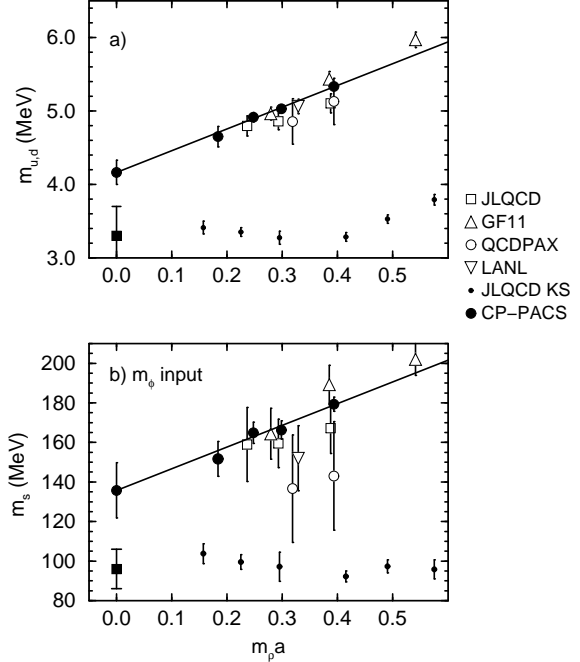

Figure 15. Values of the average of up and down quark masses (top figure) and the strange quark mass (bottom figure). They are determined perturbatively in the $\overline{MS}$ scheme at $\mu = 2$ GeV. Data of hadron masses for Wilson quarks are taken from JLQCD[8], GF11[3], QCDPAX[2] and LANL[4] to calculate quark masses by the same method we employed for the CP-PACS data. Results of quark masses for the KS action are taken from JLQCD[12]. Solid squares at $m_\rho a = 0$ represent best estimates in ref.[23] for the Wilson action in the continuum limit.

7. Decay constants

Determination of hadronic matrix elements often suffers from uncertainties in renormalization factors. An exceptional case is the vector meson decay constant f_V for which the renormalization constant for the local vector current V^L can be precisely determined non-perturbatively with the use of the conserved current V^C [20]. It has been noted by the QCDPAX Collaboration that this determination of the renormalization factor leads to a remarkable scaling of the decay constants[2].

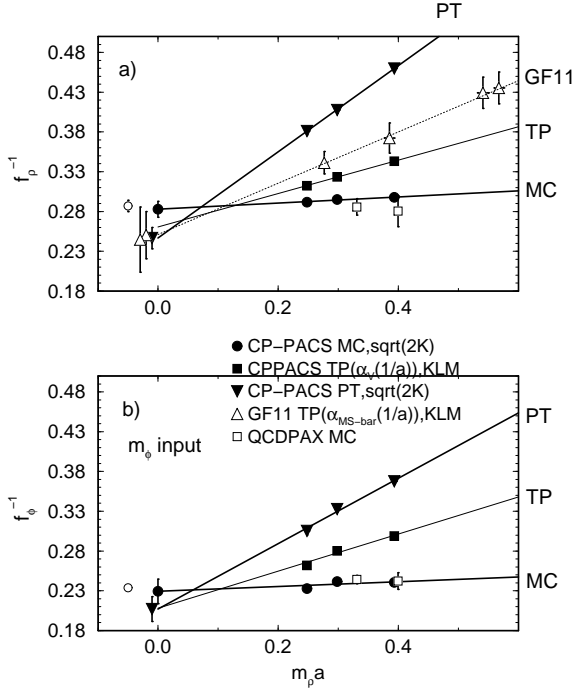In Fig.16 we plot f_V obtained with the renor-

Figure 16. Results of f_ρ and f_ϕ obtained with various renormalization constants. GF11 results [24] are plotted for comparison.

Figure 17. The same as Fig.16 for pseudo-scalar meson decay constants f_π and f_K.

malization factor calculated non-perturbatively through $Z_V = 2K\tilde{Z}_V$ with $\tilde{Z}_V$ determined from $\langle V^C|V^L\rangle/\langle V^L|V^L\rangle$. Results obtained with naive perturbative Z factor to one loop given by $Z_V = 2K(1-2.19\,\alpha_{latt.})$[22] and with tadpole-improved perturbation theory $Z_V = (1 - 3K/4K_c)(1 - 0.82\,\alpha_V(1/a))$ [10,25] are also shown for comparison.

Making a linear extrapolation of the non-perturbative result in $m_\rho a$, we obtain a value in the continuum limit which is completely consistent with experiment. Perturbative renormalization factors lead to slightly smaller values. It is worth noting that non-perturbative renormalization constant has a small value in the range of our data, given by $\tilde{Z}_V \approx 0.54$, 0.60, and 0.64 at $\beta = 5.9$, 6.1, and 6.25, respectively. A reliable extrapolation of the decay constants with one-loop evaluation of renormalization factors may be difficult in such a situation.
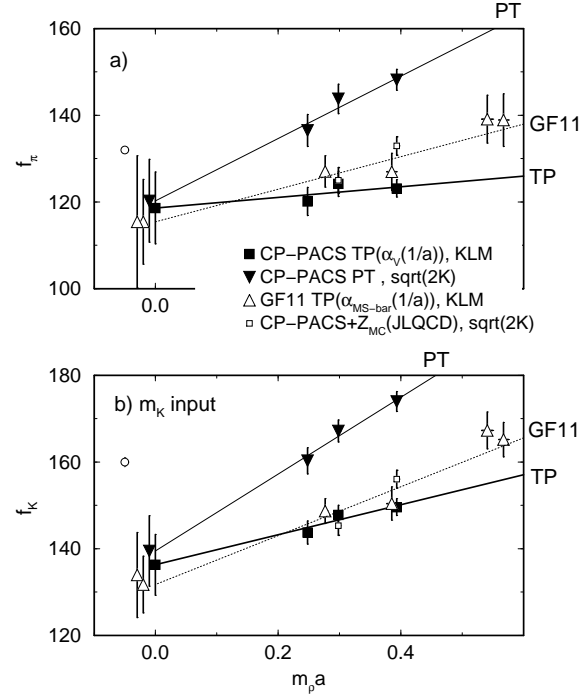
For pseudo-scalar meson decay constant f_P,

the naive one-loop perturbative Z factor takes the form $Z_A = 2K(1 - 1.68\,\alpha_{latt.})$ [22] and a tadpole-improved value is given by $Z_A = (1 - 3K/4K_c)(1 - 0.316\,\alpha_V(1/a))$ [10,25]. Both of these renormalization constants lead to a consistent value in the continuum limit as shown in Fig.17. Values of f_π and f_K in the continuum limit are smaller than the experimental values by one to two standard deviations.

A non-perturabtive estimate of the axial vector renormalization factor is available at $\beta = 5.9$ and 6.1[26,27]. Extrapolations of our data with these results for non-perturbative Z_A seems to give a consistent value with that with perturbative Z_A.

8. Conclusions

In this article we have presented a status report of our effort toward precision results of light hadron spectrum in quenched QCD with the standard plaquette and Wilson quark actions.

Our results have confirmed that strange quark

mass cannot be tuned in quenched QCD so that both pseudo scalar and vector spectra are in agreement with experiment. This observation is extended to the strange baryon sector in the present study, where our values for the baryon masses are systematically lower than experiment.

We have also found that the nucleon mass decreases faster than a linear behavior in quark mass toward the chiral limit. As a result the continuum value is smaller than the experiment, contrary to results of previous studies, albeit the difference is still a one standard deviation effect.

Finally, we have shown that quark mass determined from the axial Ward identity agrees with that from perturbation theory in the continuum limit, providing a handle for controlling the continuum extrapolation.

In parallel with these points of physics, an important lesson we would like to draw from the present work is the importance of precision; with errors down to a percent level uncertainties in physics implications can be much removed.

Encouraged by the results, we plan to further increase statistics of the three runs at β =5.9, 6.1 and 6.25. In addition we shall soon have results from the run at $\beta = 6.47$. We hope that results from the additional simulations help solidify our findings so far, and lead to a standard of the quenched hadron spectrum in QCD.

Acknowledgements

REFERENCES

1. Ape Collaboration (S. Cabasino *et al.*), Phys. Lett. B258 (1991) 195.
2. QCDPAX Collaboration (Y. Iwasaki *et al.*), Phys. Rev. D53 (1996) 6443.
3. F. Butler, H. Chen, J. Sexton, A. Vaccarino and D. Weingarten, Nucl. Phys. B430 (1994) 179.
4. T. Bhattacharya, R. Gupta, G. Kilcup and S. Sharpe, Phys. Rev. D53 (1996) 6486.
5. S. Gottlieb for MILC Collaboration, these proceedings.
6. CP-PACS Collaboration (presented by Y. Iwasaki), this volume.
7. S. Anzaki *et al.*, in preparation.
8. JLQCD Collaboration (S. Aoki *et al.*), Nucl. Phys. B (Proc. Suppl.) 53 (1997) 355.
9. S. R. Sharpe, Phys. Rev. D41 (1990) 3233; *ibid.* D46 (1992) 3146; C. Bernard and M. Golterman, *ibid.* D46 (1992) 853.
10. G. P. Lepage and P. B. Mackenzie, Phys. Rev. D48 (1993) 2250.
11. A. X. El-Khadra *et al.*, Phys. Rev. Lett. 69 (1992) 729.
12. JLQCD Collaboration (S. Aoki *et al.*), Nucl. Phys. B (Proc. Suppl.) 53 (1997) 341.
13. G. S. Bali and K. Schilling, Phys. Rev. D47 (1993) 661.
14. UKQCD Collaboration (P. Lacock and C. Michael), Phys. Rev. D52 (1995) 5213.
15. JLQCD Collaboration (S. Aoki *et al.*), Nucl. Phys. B (Proc. Suppl.) 47 (1996) 354.
16. JLQCD Collaboration (presented by S. Hashimoto), this volume.
17. For a review, see P. B. Mackenzie, Nucl. Phys. B (Proc. Suppl.) 53 (1997) 23.
18. M. Bochicchio *et al.*, Nucl. Phys. B262 (1985) 331.
19. S. Itoh, Y. Iwasaki, Y. Oyanagi and T. Yoshié, Nucl.Phys. B274 (1986) 33.
20. L. Maiani and G. Martinelli, Phys. Lett. B178 (1986) 265.
21. A. Gonzalez Arroyo, G. Martinelli and F. J. Yndurain, Phys. Lett B117 (1992) 437.
22. G. Martinelli and Y. C. Zhang, Phys. Lett. B123 (1983) 433.
23. R. Gupta and T. Bhattacharya, Los Alamos preprint LAUR-96-1840 (hep-lat/9605039); Nucl. Phys. B (Proc. Suppl.) 53 (1997) 292.
24. F. Butler, H. Chen, J. Sexton, A. Vaccarino and D. Weingarten, Nucl. Phys. B421 (1994) 217.
25. G. P. Lepage, Nucl. Phys. B (Proc.Suppl.) 26 (1992) 45; A. S. Kronfeld, Nucl. Phys. B (Proc.Suppl.) 30 (1993) 445; P. B. Mackenzie, Nucl. Phys. B (Proc.Suppl.) 30 (1993) 35.

26. JLQCD Collaboration (S.Aoki, et al.),
    Nucl. Phys. B (Proc. Suppl.) 53 (1997) 349.
27. JLQCD Collaboration (S.Aoki, et al.),
    Nucl. Phys. B (Proc. Suppl.) 53 (1997) 209.